

Supplementary Information

Active $\text{Cu}_x\text{Co}_{1-x}\text{Al}_2\text{O}_4$ spinel catalysts with potent SO_2 tolerance for toluene combustion: Measuring Cu substitution capacity in spinel lattice with XRD extrapolation

Junhua Cao^a, Haojun Liu^a, Shijing Zhang^{a,*}, Teng Liu^a, Yu Lv^a, Zhiqiang Wu^a, Xianglan Xu^a, Junwei Xu^b, Xiuzhong Fang^a, Xiang Wang^{a,*}

a. Key Laboratory of Jiangxi Province for Environment and Energy Catalysis, School of Chemistry and Chemical Engineering, Nanchang University, Nanchang, Jiangxi, 330031 (P.R. China)

b. Department of Applied Chemistry, Jiang Xi Academy of Science, Nanchang, 330096, China.

** Corresponding authors. E-mail addresses: xwang23@ncu.edu.cn (X. Wang), sjzhang230@163.com (S. J. Zhang)*

1. Supplementary Experimental

1.1 Catalyst characterization

The Powder X-ray diffraction (XRD) patterns were recorded on a Bruker AXS D8 Focus diffractometer instrument operating at 40 kV and 30 mA, with Cu target $K\alpha$ -ray irradiation ($\lambda = 1.5405 \text{ \AA}$). Scans were taken with a 2θ range from 10 – 90° and a step of 4° min^{-1} . To keep the data comparable, all the samples were tested continuously.

Raman spectra were tested using an excitation wavelength of 532 nm in Renishaw in Via instrument equipped with an argon laser excitation source. The scanned Raman shift range is from 100 to 1400 cm^{-1} .

The FTIR spectra were recorded in the range of 4000 – 400 cm^{-1} using a Bruker Vertex equipped with an MCT detector. Prior to the measurements the samples were homogenized with KBr by using an agate mortar, and then pressed into thin and transparent pellets. Hooke's law from $\nu = \sqrt{k/\mu}/2\pi c$, where c , k and μ are light speed, bond force constant and effective mass¹.

Scanning electron microscopy (SEM) images were recorded on a Hitachi S-4800 field emission scanning electron microscope. Transmission electron microscopy (TEM) and high-resolution transmission electron microscopy (HRTEM) images were recorded on a TecnaiTM F30 transmission electron microscope. Elemental phase mapping and surface scans were also obtained by energy-dispersive spectroscopy (EDX) using the TecnaiTM F30 microscope equipped with an Oxford EDX detector operated at 300 keV .

The specific surface areas were measured by N_2 sorption at 77 K on an ST-08B instrument.

Hydrogen temperature programmed reduction (H_2 -TPR) tests were performed on the FINESORB 3010C automatic temperature programmed chemical adsorption instrument of Zhejiang Fantai. Firstly, 50 mg catalyst was pretreated in the $99.9\% \text{ Ar}$ flow at 120° C for 30 min and then cooled to room temperature. The treatment gas was switched to a $10\% \text{ H}_2/\text{Ar}$ mixture. After the baseline was stabilized, the catalyst bed is raised from room temperature to 800° C at a heating rate of $10^\circ \text{ C min}^{-1}$, and the thermal conductivity detector (TCD) to detect and record.

O₂ temperature-programmed desorption (O₂-TPD) measurements were carried out on Micromeritics Auto Chem 2920 chemical adsorption instrument with a TCD. Typically, 50 mg sample was placed in a quartz reactor, which was pretreated in a 30 mL min⁻¹ 99.99% He flow at 600 °C for 60 min. Afterwards, the sample was cooled down to 50 °C and saturated in a 3% O₂/He flow with a rate of 30 mL min⁻¹ for 1 h, which was followed by purging with a 30 mL min⁻¹ 99.99% He flow for 30 min to remove any physically adsorbed O₂. Temperature-programmed desorption experiments were then carried out from 50 to 800 °C with a heating rate of 10 °C min⁻¹ in a 30 mL min⁻¹ 99.99% He flow.

Electron Paramagnetic Resonance (EPR) has been used to measure the catalysts. The catalysts were pretreated in 100 Torr oxygen at 750 °C for 1 h and then cooled down to room temperature, which was followed by evacuation and then placed in liquid nitrogen of 77 K prior to record the EPR signals. Afterwards, the EPR spectra were recorded with a JEOL FA-200 EPR Spectrometer, operating with a field modulation of 100 kHz and microwave frequencies of 9067.558 MHz.

X-ray Photoelectron Spectroscopy (XPS) tests were performed with a PerkinElmer PHI1600 system using a single MgK α X-ray source operated at 300 W and 15 kV voltage. The spectra were collected at room temperature with an ultra-high vacuum. The binding energies were calibrated by using the C 1s peak of graphite at 284.8 eV as a standard.

In situ DRIFTS experiments were carried on a Bruker Vertex equipped with an MCT detector chilled in liquid nitrogen. A micro-size In Situ DRIFTS furnace equipped with KBr windows was used. 100 mg powder sample was pretreated at 500 °C for 60 min in a high purity 30 mL min⁻¹ Ar flow and then cooled target temperature. At this stage, the background spectra were collected at a resolution of 4 cm⁻¹ by accumulating 64 scans in a 30 mL/min Ar flow. All the spectra exhibited in this study were achieved by subtracting the corresponding background spectrum. The spectra were recorded continuously for each series of in situ experiments until the reaction reached equilibrium, which is about 2 min.

NH₃ temperature programmed desorption (NH₃-TPD) was performed on the DAS-7000 temperature programmed chemical adsorption instrument of HUASI. Typically, 50 mg catalyst was pretreated in a 30 mL/min 99.99% He flow at 400 °C 1h to remove any possible impurities and H₂O. Afterwards, the sample was cooled to 50 °C and

adsorb NH_3 for 1 h was followed by purging with a 30 mL/min 99.99% He flow to remove any physically absorbed toluene for 30 min. After all these pretreatments, the catalyst was heated from 50 to 800 °C with a rate of 10 °C /min. A TCD was employed to monitor the NH_3 desorption.

Toluene temperature programmed desorption (Toluene-TPD) was performed on the DAS-7000 temperature programmed chemical adsorption instrument of HUASI. Typically, 50 mg catalyst was pretreated in a 30 mL/min high purity He flow at 400 °C 1h to remove any possible impurities and H_2O . Afterwards, the sample was cooled to 50 °C and adsorb toluene for 1 h was followed by purging with a 30 mL/min 99.99% He flow to remove any physically absorbed toluene for 30 min. After all these pretreatments, the catalyst was heated from 50 to 800 °C with a rate of 10 °C /min. A TCD was employed to monitor the toluene desorption.

All calculations in this work were performed using density functional theory (DFT) with the Vienna Ab Initio Simulation Package (VASP). The Perdew-Burke-Ernzerhof (PBE) functional within the generalized gradient approximation (GGA) was used for the exchange-correlation energy. Electron-ion interactions were treated using the Projector Augmented Wave (PAW) method. To reduce interactions between periodic images in slab model calculations, a 15 Å vacuum spacing was introduced, and dipole correction was applied with summarization turned off. Based on convergence tests of total energy, the cutoff energy was set at 450 eV for all structures. Convergence criteria were established for the self-consistent field (1.0×10^{-6} eV/atom), energy (1.0×10^{-5} eV/atom), force (0.03 eV/Å), atomic displacement (1.0×10^{-3} Å), and stress components (0.05 GPa).

O_2 Defect energy calculations followed the formula:

$$E_V = E_{\text{defect}} - E_{\text{bulk}} + 1/2 E_{\text{O}_2}$$

where E_{def} is the total energy of the structure with the oxygen vacancy; E_{bulk} is the total energy of the perfect crystal structure; E_{O_2} is the total energy of an oxygen molecule.

1.2 Activity evaluation

The samples were evaluated for CO oxidation with a fixed bed reactor. The volume composition of the feed gas is 1% CO, 21% O_2 and balanced by N_2 , with a total flow rate of 30 mL min^{-1} . Generally, 0.05 g sample was used for activity evaluation,

which resulted in a WHSV of 36000 mL g⁻¹·h⁻¹. A K-type thermocouple was placed on top of the catalyst bed with the head point touching the sample to monitor the accurate reaction temperatures. To measure the light-off behaviors of the catalysts, all data were collected by increasing the temperature. The reactants and products were analyzed on-line on a GC9310 gas chromatograph equipped with a TDX-01 column and a TCD detector. Before analysis, the reaction at each temperature over the catalysts was stabilized at least 30 min.

The catalysts were evaluated for toluene deep oxidation in a quartz tube (ID = 6 mm) reactor with a continuous flow over 0.05 g catalyst fix the same weight silica sand. Typically, 0.3-0.4 mm catalyst particles were used for activity evaluation. A K-type thermocouple was placed inside the catalyst bed with the thermocouple head point touching the catalyst bed to monitor the reaction temperature accurately. To measure the light-off behaviors of the catalysts, all data were collected with increasing the temperature. The volume composition of the feed gas is 1000 ppm toluene + 99.99% air. The flow rate is 30 mL min⁻¹, which corresponds to a space velocity of 36000 mL h⁻¹ g⁻¹ cat. The 1000 ppm toluene was generated by passing air flow through a bottle containing pure toluene that was chilled in an alcohol low-temperature isothermal bath controlled at -30 °C. The reactants and products were analyzed on-line on a SP7890 gas chromatograph equipped with a flame ionization detector (FID) and a TCD, using a SE-30 capillary column (15 m in length) for VOCs separation and a TDX-01 column (3 mm in diameter and 3 m in length) for the separation of O₂, N₂ and CO₂. Before analysis, the reaction was stabilized at each temperature for at least 30 min to get steady state kinetic data. The flow rate of the H₂ carrier gas is 30 mL min⁻¹. The selectivity for CO₂ in this study was above 98%, so we identified that the converted toluene at each temperature is completely oxidized.

2. Supplementary Results

Table S1. XRD, N₂-BET and FTIR results.

Catalyst	Crystallite size ^a (nm)	Specific surface area (m ² g ⁻¹)	Co–O bond wavenumber (cm ⁻¹)	Bond force constant K (N·cm ⁻¹) ^b	Al–O bond wavenumber (cm ⁻¹)	Bond force constant K (N·cm ⁻¹) ^b
CoAl ₂ O ₄	33.9	12	635	2.97	817	3.93
Cu _{0.1} Co _{0.9} Al ₂ O ₄	33.8	10	633	2.95	815	3.91
Cu _{0.3} Co _{0.7} Al ₂ O ₄	25.2	15	631	2.93	812	3.88
Cu _{0.5} Co _{0.5} Al ₂ O ₄	24.6	14	628	2.91	810	3.86
Cu _{0.7} Co _{0.3} Al ₂ O ₄	23.2	14	–	–	806	3.82
Cu _{0.9} Co _{0.1} Al ₂ O ₄	18.6	13	–	–	803	3.79
CuAl ₂ O ₄	17.9	12	–	–	801	3.77

^a Calculated by Scherrer equation with the (311) facet of CoAl₂O₄.

^b Calculated by Hooke's law. See the details in the experimental of FTIR.

Table S2 Activity comparison of the optimal $\text{Cu}_{0.5}\text{Co}_{0.5}\text{Al}_2\text{O}_4$ catalyst in this study with some typical results published in literatures

Catalyst	Toluene (ppm)	WHSV ($\text{mL}\cdot\text{g}^{-1}\cdot\text{h}^{-1}$)	Toluene combustion temperature T_{90} ($^{\circ}\text{C}$)	Reference
$\text{Cu}_{0.5}\text{Co}_{0.5}\text{Al}_2\text{O}_4$	1000	36000	290	This work
CuAl_2O_4	1000	36000	350	2
$\text{CuMn}_2\text{O}_4\text{-AT}$	1000	60000	245	3
CuCo_2O_4	1000	78000	230	4
$\text{CoMn}_2\text{O}_4\text{-SGC}$	-	3750 h^{-1}	340	5
$\text{Ru}/m\text{-HZSM-5(3)}$	40	80000	243	6
Cu1.0Mn1.5/Al	1000	120000 h^{-1}	293	7
LaNiO_3	4000	47000 h^{-1}	305	8
AlCo_3O	1000	60000	325	9
1.2% $\text{Ru/Pr}_2\text{Sn}_2\text{O}_7$	1000	36000	280	10
SiBEACo7.0	1000	60000	322	11

Table S3 Quantified H₂-TPR and O₂-TPD results

Catalyst	H ₂ uptake amount (mmol g ⁻¹)			O ₂ desorption amount (μmol g ⁻¹)		
	α	β	total	α	β	total
CoAl ₂ O ₄	-	-	-	3.41	3.06	6.47
Cu _{0.1} Co _{0.9} Al ₂ O ₄	0.04	-	0.04	4.58	2.81	7.39
Cu _{0.3} Co _{0.7} Al ₂ O ₄	0.31	-	0.31	7.65	3.02	10.67
Cu _{0.5} Co _{0.5} Al ₂ O ₄	0.47	-	0.47	9.59	4.57	14.16
Cu _{0.7} Co _{0.3} Al ₂ O ₄	0.70	-	0.70	6.99	3.93	10.92
Cu _{0.9} Co _{0.1} Al ₂ O ₄	1.26	2.01	3.27	6.38	4.19	10.57
CuAl ₂ O ₄	1.34	2.64	3.98	4.75	4.60	9.35

Table S4 XPS O 1s quantification results

Catalyst	O 1s binding energy (eV) and relative amount (a.u.)			
	O ²⁻	CO ₃ ²⁻ /OH ⁻	O ₂ ⁻	O ₂ ⁻ /O ²⁻ ratio
CoAl ₂ O ₄	530.54/0.59	530.85/0.20	531.82/0.21	0.36
Cu _{0.1} Co _{0.9} Al ₂ O ₄	530.50/0.57	531.24/0.20	531.88/0.23	0.40
Cu _{0.3} Co _{0.7} Al ₂ O ₄	530.10/0.52	530.93/0.23	531.60/0.25	0.48
Cu _{0.5} Co _{0.5} Al ₂ O ₄	530.22/0.52	530.78/0.20	531.50/0.28	0.54
Cu _{0.5} Co _{0.5} Al ₂ O ₄ (s) ^a	530.70/0.55	531.20/0.18	531.80/0.27	0.49
Cu _{0.7} Co _{0.3} Al ₂ O ₄	530.60/0.53	531.23/0.19	531.85/0.28	0.53
Cu _{0.9} Co _{0.1} Al ₂ O ₄	530.58/0.52	531.18/0.24	531.85/0.24	0.46
CuAl ₂ O ₄	530.40/0.52	531.05/0.25	531.50/0.23	0.44

^a Cu_{0.5}Co_{0.5}Al₂O₄ catalyst after sulfur tolerance test

Table S5 Quantified NH₃-TPD and Toluene-TPD results

Catalyst	Relative NH ₃ desorption amount (a.u.)	Relative toluene desorption amount (a.u.)
CoAl ₂ O ₄	20	57
Cu _{0.1} Co _{0.9} Al ₂ O ₄	24	62
Cu _{0.3} Co _{0.7} Al ₂ O ₄	51	76
Cu _{0.5} Co _{0.5} Al ₂ O ₄	100	100
Cu _{0.7} Co _{0.3} Al ₂ O ₄	59	89
Cu _{0.9} Co _{0.1} Al ₂ O ₄	41	72
CuAl ₂ O ₄	32	71

Table S6 CO oxidation kinetic data on $\text{Cu}_x\text{Co}_{1-x}\text{Al}_2\text{O}_4$ catalysts

Catalyst	R_w (10^{-4} mmol·g ⁻¹ s ⁻¹) ^a	R_s (10^{-5} mmol s ⁻¹ m ⁻²) ^a	E_a (kJ mol ⁻¹)
CoAl_2O_4	1.4	1.2	60
$\text{Cu}_{0.1}\text{Co}_{0.9}\text{Al}_2\text{O}_4$	2.2	2.2	59
$\text{Cu}_{0.3}\text{Co}_{0.7}\text{Al}_2\text{O}_4$	4.5	3.0	54
$\text{Cu}_{0.5}\text{Co}_{0.5}\text{Al}_2\text{O}_4$	7.4	5.3	50
$\text{Cu}_{0.7}\text{Co}_{0.3}\text{Al}_2\text{O}_4$	5.3	3.8	53
$\text{Cu}_{0.9}\text{Co}_{0.1}\text{Al}_2\text{O}_4$	3.8	2.9	55
CuAl_2O_4	2.9	2.4	55

^a R_w and R_s , differential rates normalized by catalyst mass or surface area at 150 °C

Table S7 Quantified O₂-TPD results of the fresh and spent Cu_{0.5}Co_{0.5}Al₂O₄ catalyst

Catalyst	O ₂ desorption amount (μmol g ⁻¹)		
	α	β	total
fresh-Cu _{0.5} Co _{0.5} Al ₂ O ₄	9.59	4.57	14.16
spent-Cu _{0.5} Co _{0.5} Al ₂ O ₄	9.85	7.47	17.32

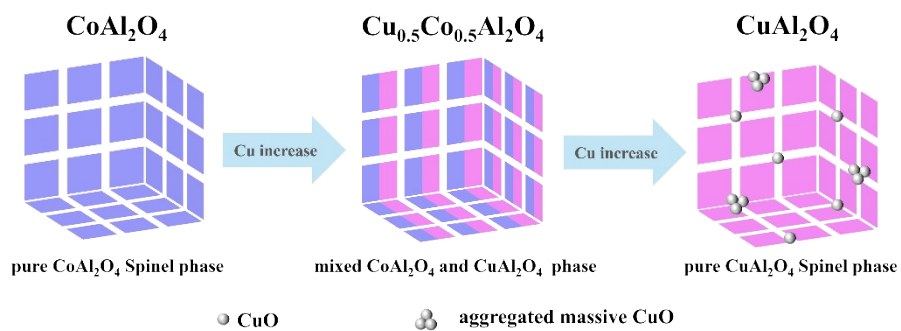


Fig. S1 Structure change diagram of $\text{Cu}_x\text{Co}_{1-x}\text{Al}_2\text{O}_4$ catalysts with the increasing of CuO content.

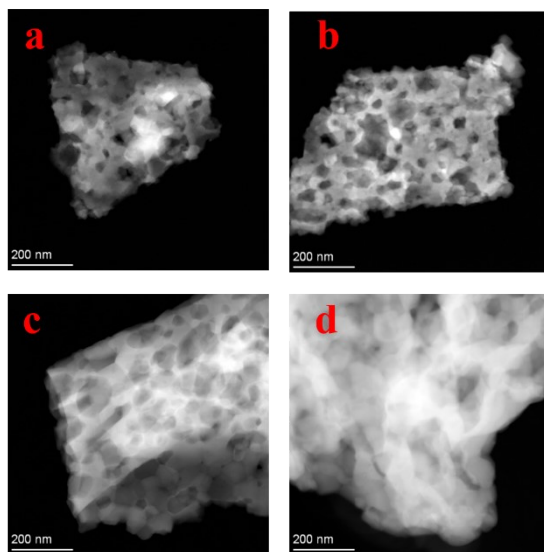


Fig. S2 STEM pictures of (a) $\text{Cu}_{0.9}\text{Co}_{0.1}\text{Al}_2\text{O}_4$. (b) $\text{Cu}_{0.5}\text{Co}_{0.5}\text{Al}_2\text{O}_4$. (c) $\text{Cu}_{0.1}\text{Co}_{0.9}\text{Al}_2\text{O}_4$. (d) CoAl_2O_4 .

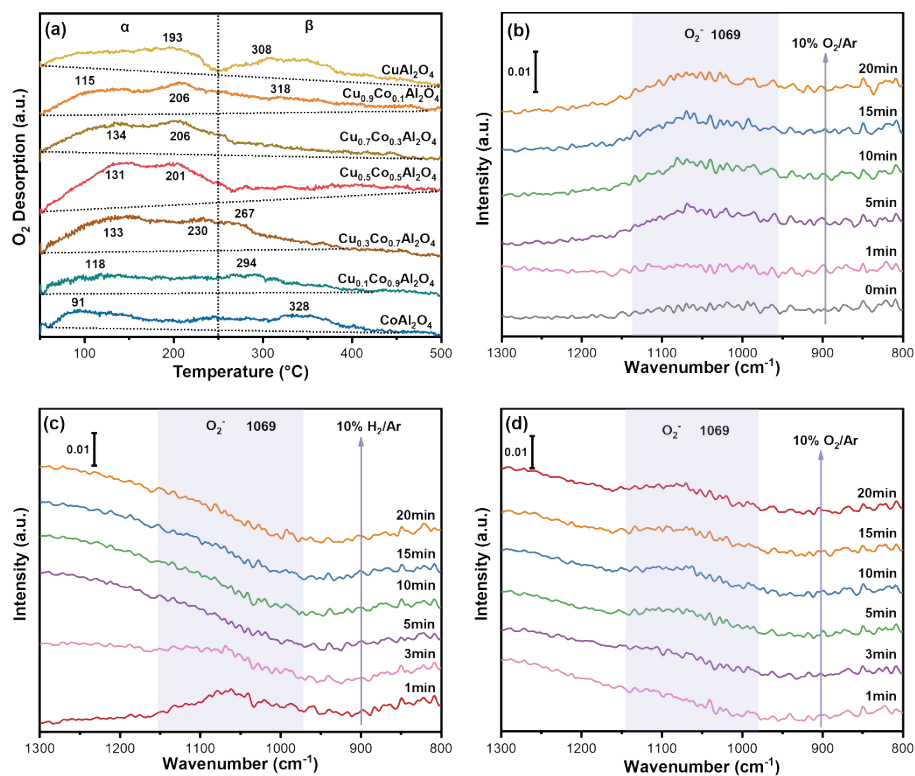


Fig. S3 (a) O₂-TPD profiles of Cu_xCo_{1-x}Al₂O₄ catalysts. *In situ* DRIFTS studies of Cu_{0.5}Co_{0.5}Al₂O₄ at 300 °C (b) in a 10% O₂/Ar stream. (c) switch to a 10% H₂/Ar stream and (d) switched back to 10% O₂/Ar stream.

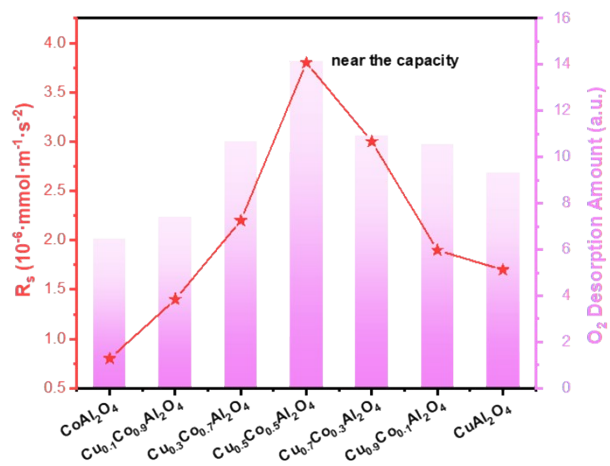


Fig. S4 The relationship between O_2 desorption amount (O_2 -TPD) and R_s at 220 °C.

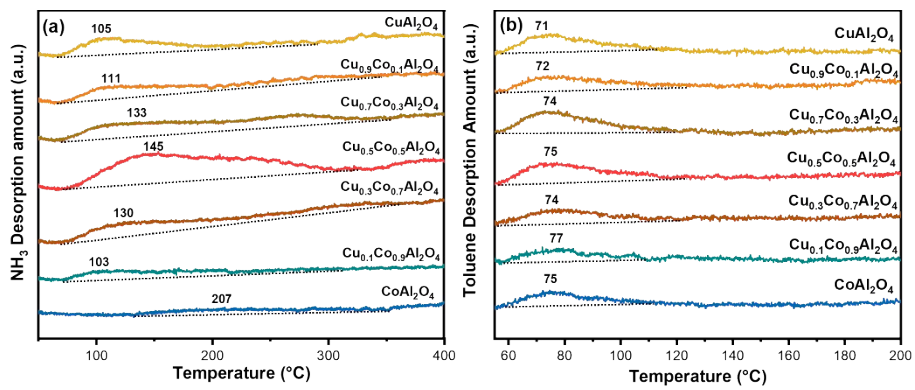


Fig. S5 (a) NH_3 -TPD and (b) Toluene-TPD profiles of $\text{Cu}_x\text{Co}_{1-x}\text{Al}_2\text{O}_4$ catalysts.

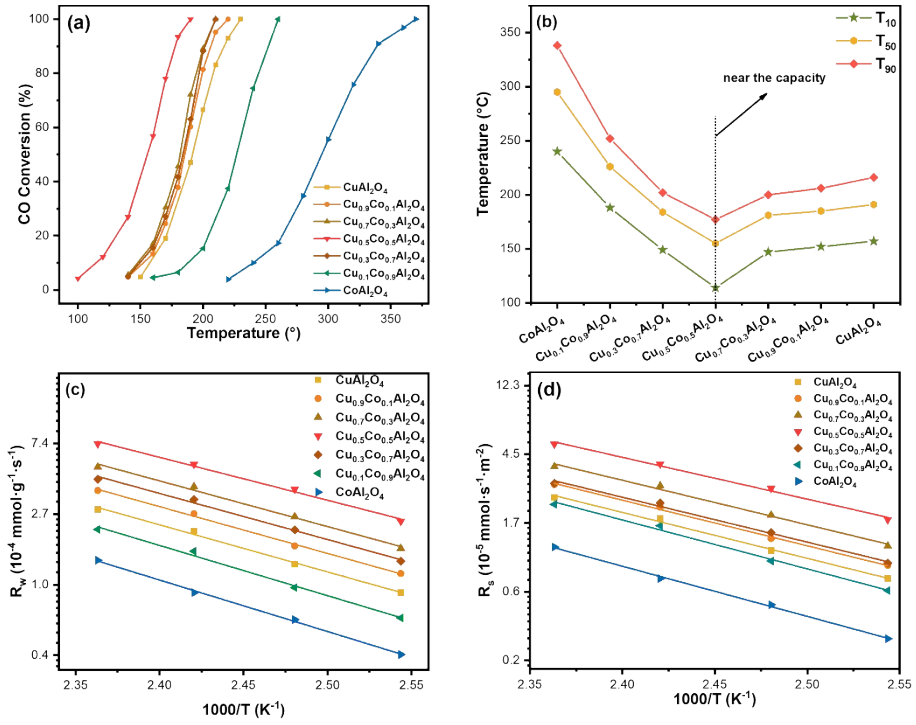


Fig. S6 CO oxidation activity on $\text{Cu}_x\text{Co}_{1-x}\text{Al}_2\text{O}_4$ catalysts. (a) CO conversion. (b) T_{10} , T_{50} and T_{90} . (c) Arrhenius plots based on R_w . (d) Arrhenius plots based on R_s .

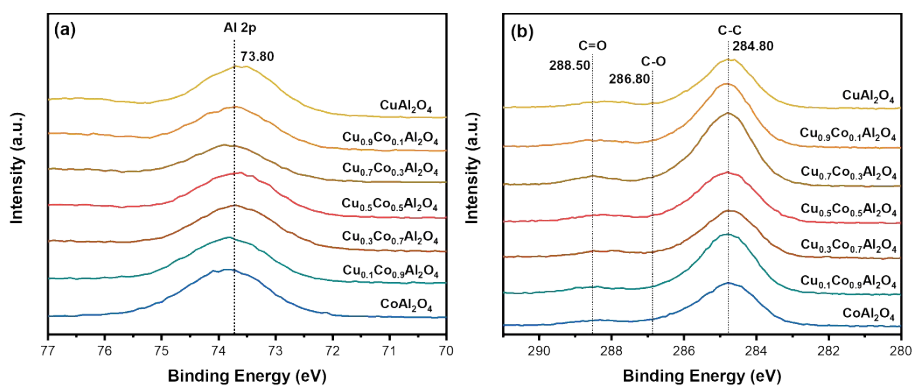


Fig. S7 XPS analysis of $\text{Cu}_x\text{Co}_{1-x}\text{Al}_2\text{O}_4$ catalysts. (a) Al 2p spectra. (b) C 1s spectra.

The C 1s standard peak is observed at 284.8 eV. The two characteristic diffraction peaks at 288.5 eV and 286.8 eV are attributed to the vibrations of C=O and C-O bonds, respectively, indicating the presence of carbonate species on the catalyst surface.

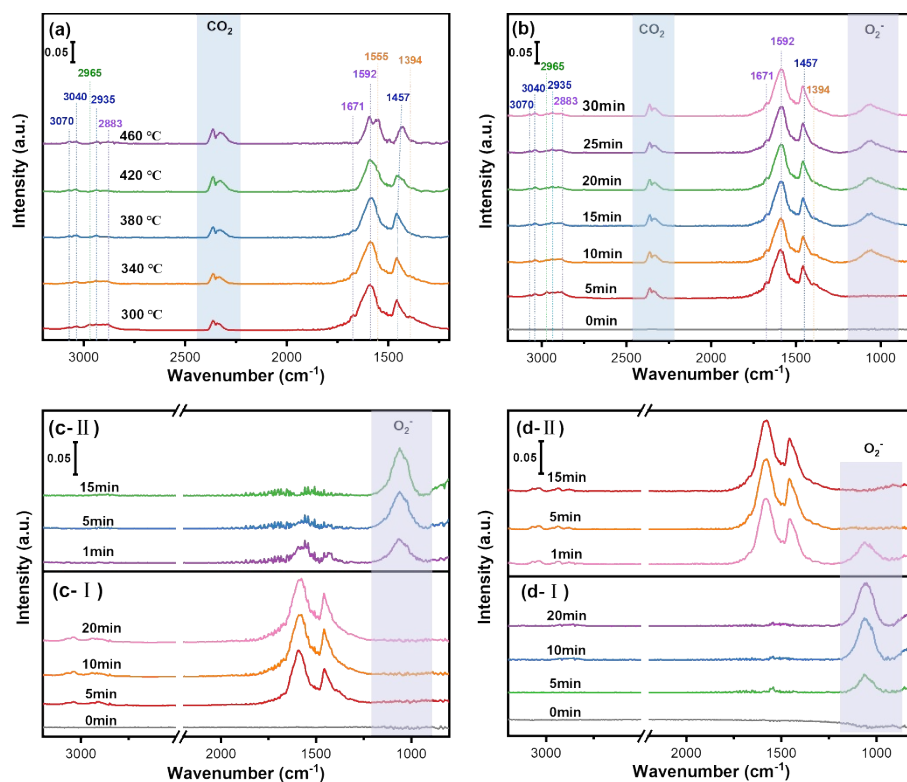


Fig. S8 *In-situ* DRIFTS experiments on CoAl_2O_4 (a) In the reaction feed consisting of 1000 ppm toluene+10% O_2/Ar at different temperature. (b) In the reaction feed consisting of 1000 ppm toluene and 10% O_2/Ar at 340 °C. (c-I) In 1000 ppm toluene/ Ar flow at 340 °C. (c-II) In the 10% O_2/Ar flow at 340 °C. (d-I) In the 10 % O_2/Ar flow at 340 °C. (d-II) In 1000 ppm toluene/ Ar flow at 340 °C.

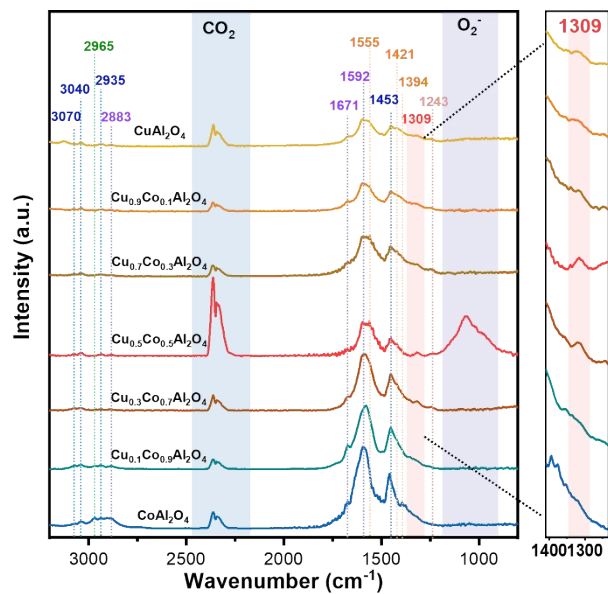


Fig. S9 *In situ* DRIFTS spectra of $\text{Cu}_x\text{Co}_{1-x}\text{Al}_2\text{O}_4$ catalysts in the reaction consisting of 1000 ppm toluene + 10% O_2/Ar feed at 300 °C.

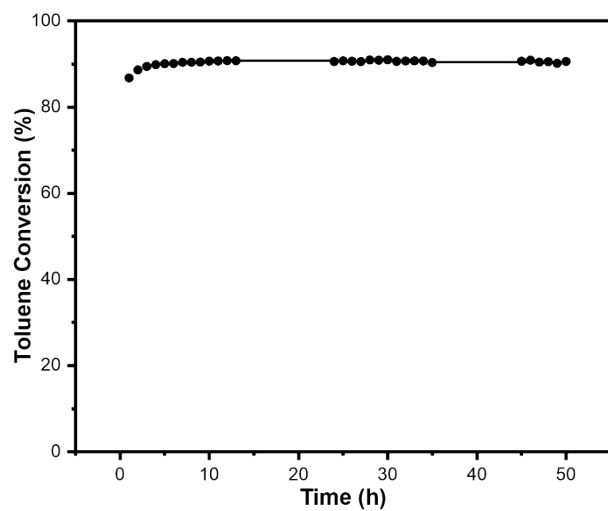


Fig. S10 The reaction stability test of $\text{Cu}_{0.5}\text{Co}_{0.5}\text{Al}_2\text{O}_4$ sample.

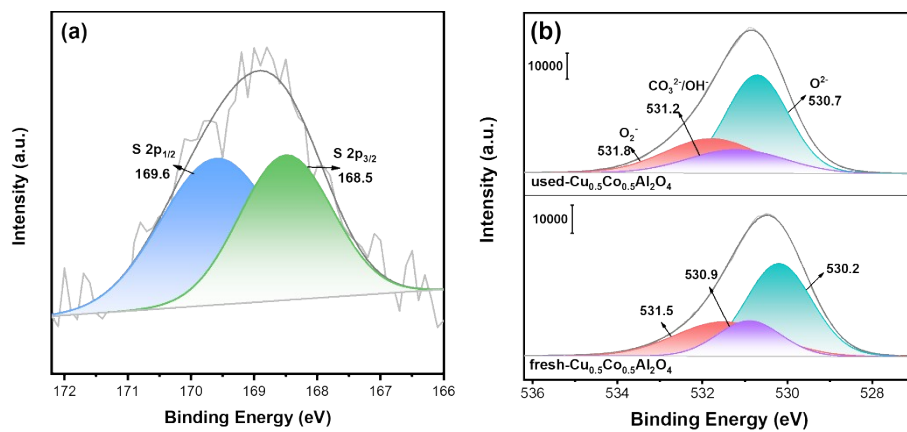


Fig. S11 XPS analysis of fresh $\text{Cu}_{0.5}\text{Co}_{0.5}\text{Al}_2\text{O}_4$ and the spent catalyst after sulphur tolerance test. (a) S 2p spectra. (b) O 1s spectra.

References

1. S. Kaya, C. Kaya, I. B. Obot and N. Islam, A novel method for the calculation of bond stretching force constants of diatomic molecules, *Spectrochim. Acta. A Mol. Biomol. Spectrosc.*, 2016, **154**, 103-107.
2. L. Yu, Y. Haiming, L. Teng, X. Junwei, X. Xianglan, F. Xiuzhong and W. Xiang, Manufacturing AAl_2O_4 (A=Cu, Co, Ni, Zn) Spinel Catalysts for Toluene Combustion: Elucidating the A-site Replacement Effect on the Reactivity, *ChemCatChem*, 2024, **16**.
3. Y. Yang, W. Si, Y. Peng, Y. Wang, H. Liu, Z. Su and J. Li, Defect Engineering on $CuMn_2O_4$ Spinel Surface: A New Path to High-Performance Oxidation Catalysts, *Environ. Sci. Technol.*, 2022, **56**, 16249-16258.
4. K. Li, T. Li, Y. Dai, Y. Quan, J. Zhao and J. Ren, Highly active urchin-like MCo_2O_4 (M = Co, Cu, Ni or Zn) spinel for toluene catalytic combustion, *Fuel*, 2022, **318**, 123648.
5. S. A. Hosseini, D. Salari, A. Niaei, F. Deganello, G. Pantaleo and P. Hojati, Chemical-physical properties of spinel $CoMn_2O_4$ nano-powders and catalytic activity in the 2-propanol and toluene combustion: Effect of the preparation method, *J. Environ. Sci. Health Part A*, 2011, **46**, 291-297.
6. Y. Wang, D. Yang, S. Li, M. Chen, L. Guo and J. Zhou, Ru/hierarchical HZSM-5 zeolite as efficient bi-functional adsorbent/catalyst for bulky aromatic VOCs elimination, *Micropor. Mesopor. Mater.*, 2018, **258**, 17-25.
7. H. Wang, Y. Lu, Y. Han, C. Lu, H. Wan, Z. Xu and S. Zheng, Enhanced catalytic toluene oxidation by interaction between copper oxide and manganese oxide in Cu-O-Mn/ γ - Al_2O_3 catalysts, *Appl. Surf. Sci.*, 2017, **420**, 260-266.
8. G. Pecchi, M. G. Jiliberto, E. J. Delgado, L. E. Cadús and J. L. G. Fierro, Effect of B-site cation on the catalytic activity of $La_{1-x}Ca_xBO_3$ (B = Fe, Ni) perovskite-type oxides for toluene combustion, *J. Chem. Technol. Biotechnol.*, 2011, **86**, 1067-1073.
9. W. Tu, X. Dong, R. Du, Q. Wang, F. Yang, R. Ou, X. Wang, L. Li and A. Yuan, Hierarchical laminated Al_2O_3 in-situ integrated with high-dispersed Co_3O_4 for improved toluene catalytic combustion, *Adv. Powder Technol.*, 2022, **33**, 103377.
10. J. Liu, L. Zeng, X. Xu, J. Xu, X. Fang, Y. Bian and X. Wang, Elucidating Ru Distribution State of Ru-Promoted $Pr_2Sn_2O_7$ Pyrochlore and its Effect on the Catalytic Performance for Toluene Deep Oxidation, *ChemCatChem*, 2022, **14**.
11. A. Rokicińska, M. Drozdek, B. Dudek, B. Gil, P. Michorczyk, D. Brouri, S. Dzwigaj and P. Kuśtrowski, Cobalt-containing BEA zeolite for catalytic combustion of toluene, *Appl. Catal. B Environ. Energy*, 2017, **212**, 59-67.